

# Long noncoding RNA MAFG-AS1 facilitates the progression of hepatocellular carcinoma *via* targeting miR-3196/OTX1 axis

Z.-Q. HU<sup>1,2</sup>, H.-C. LI<sup>2,3</sup>, F. TENG<sup>1,2</sup>, Q.-M. CHANG<sup>1,2</sup>, X.-B. WU<sup>1,2</sup>, J.-F. FENG<sup>1,2</sup>, Z.-P. ZHANG<sup>1,2</sup>

<sup>1</sup>Department of Hepatobiliary-Pancreatic Surgery, Minhang Hospital, Fudan University, Shanghai, China

<sup>2</sup>Institute of Fudan-Minhang Academic Health System, Minhang Hospital, Fudan University, Shanghai, China

<sup>3</sup>Department of Surgery, Minhang Hospital, Fudan University, Shanghai, China

*Zhiqiu Hu and Hongchang Li contributed equally to this work*

**Abstract.** – **OBJECTIVE:** Hepatocellular carcinoma (HCC) is an invasive malignant tumor with high mortality rate. Long non-coding RNA (lncRNA) MAFG-AS1 has been showed to play an oncogenic role in several malignant tumors. Nonetheless, the exact role of MAFG-AS1 in the progression of HCC has not been fully elucidated.

**PATIENTS AND METHODS:** Real-time quantitative polymerase chain reaction (RT-qPCR) and Western blot were used to detect the mRNA and protein expression of MAFG-AS1 in HCC tissues and cells. Cell counting kit-8 (CCK-8), transwell and tubule formation assays were applied to uncover the proliferation, migration, invasion and tumor angiogenesis of HCC cells, respectively. RNA binding protein immunoprecipitation (RIP) assay and Luciferase reporter gene assay were employed to explore the molecular mechanism. In addition, Xenograft assay was used to investigate the effect of MAFG-AS1 *in vivo*.

**RESULTS:** MAFG-AS1 was highly expressed in HCC tissues and cells. Attenuation of MAFG-AS1 evidently suppressed the proliferation, migration, invasion and tumor angiogenesis of HCC cells, suggesting that MAFG-AS1 played an oncogenic role in HCC. MiR-3196 was sponged by MAFG-AS1, and OTX1 was a downstream target of miR-3196 in HCC. In addition, OTX1 expression was negatively associated with miR-3196 but positively associated with MAFG-AS1 in HCC tissues. Overexpression of OTX1 could abolish the repressive influence of MAFG-AS1 inhibition on the proliferation, migration, invasion and tumor angiogenesis of HCC cells.

**CONCLUSIONS:** MAFG-AS1 facilitated the progression of HCC via targeting miR-3196/OTX1 axis, which might be used as a new insight for HCC treatment.

*Key Words:*

MAFG-AS1, MiR-3196, OTX1, Hepatocellular carcinoma (HCC).

## Introduction

Primary liver cancer is the second leading cause of death around the world<sup>1</sup>. In recent years, the incidence of liver cancer has been on the rise, with about 3% in women and 4% in men<sup>2</sup>. Hepatocellular carcinoma (HCC), the most typical subtype of primary liver cancer, possesses high morbidity and mortality worldwide<sup>3</sup>. Currently, transcatheter arterial embolization (TAE) and transcatheter chemotherapy embolization (TACE) are the primary interventional therapies for HCC patients. Hepatectomy is more effective for patients with HCC at an early stage and those with satisfactory liver function, while TACE is recommended for patients with advanced HCC<sup>4</sup>. Although it has been reported that TACE is more effective in the treatment of 3-5 cm tumors<sup>5</sup>, the long-term survival rate of patients is still far from satisfactory. TACE or TAE cannot significantly improve the survival rate of patients with liver cancer in the middle stage<sup>6</sup>. Besides, the 5-year survival rate of HCC patients is lower than 10%, which remains dismal<sup>7</sup>. Therefore, it is meaningful to explore the potential molecular mechanism of HCC development and to uncover more efficient therapeutic targets.

Long noncoding RNAs (lncRNAs) are a type of RNA transcripts implicated in various biological processes, such as cell proliferation, migration, invasion and apoptosis<sup>8,9</sup>. They serve as vital factors in malignant tumors. Of note, lncRNA LINC01197, regulated by FOXO1, inhibits the proliferation of pancreatic adenocarcinoma cells *via* inactivating Wnt/ $\beta$ -catenin signaling<sup>10</sup>. LINC00612 promotes the proliferation and invasion of bladder cancer cells *via* sponging miR-590 to upregulate PHF14 expression<sup>11</sup>. lncRNA ZEB1-AS1 promotes the migration, invasion and proliferation, and inhibits the apoptosis of bladder cancer as a competing endogenous RNA *via* elevating the expression of fascin-1 by sponging miR-200b<sup>12</sup>. HOXD-AS1 facilitates the epithelial to mesenchymal transition of ovarian cancer cells through sponging miR-186-5p and regulating PIK3R3<sup>13</sup>. lncRNA MAFG-AS1 has also been confirmed to play a significant role in several malignancies. Sui et al<sup>14</sup> has demonstrated that MAFG-AS1 aggravates the proliferation of lung adenocarcinoma cells through targeting miR-744-5p/MAFG axis. MAFG-AS1 enhances the development of breast carcinoma *via* regulating miR-339-5p/MMP15 axis<sup>15</sup>. MAFG-AS1 drives the progression of colorectal cancer by sponging miR-147b and enhancing the expression of NDUFA4<sup>16</sup>. Nevertheless, the exact role of MAFG-AS1 in the progression of HCC and the possible underlying mechanism have not been fully elucidated.

In the present study, we aimed to unveil the role and function of MAFG-AS1 in HCC progression. The results indicated that MAFG-AS1 facilitated the progression of HCC *via* targeting miR-3196/OTX1 axis. All our findings suggested that MAFG-AS1 might become a promising therapeutic target for the treatment of HCC.

## Patients and Methods

### Patients and Tissue Specimens

This investigation was approved by the Research Ethics committee of Minhang Hospital, Fudan University. HCC tissues and adjacent normal tissues were obtained from patients. The selection of patients was based on the guideline proposed by the Union for International Cancer Control (UICC). All patients did not receive adjuvant radiotherapy, chemotherapy, or immunotherapy before surgery. Informed written consent was obtained from patients before the study.

### Cell Culture

Human normal liver cell line L02 and human HCC cell lines (HCCLM3, Hep3B, Huh7 and MHCC97-H) were obtained from Shanghai Institutes for Biological Sciences, Chinese Academy of Sciences (Shanghai, China). All cells were cultured in Dulbecco's Modified Eagle's Medium (DMEM) medium (Invitrogen, Carlsbad, CA, USA) containing 100  $\mu$ g/mL streptomycin, 100 U/mL penicillin, and 10% fetal bovine serum (FBS) (Gibco, Rockville, MD, USA) in an incubator at 37°C with 5% CO<sub>2</sub>.

### Cell Transfection

Short hairpin RNA targeting MAFG-AS1 (sh-MAFG-AS1#1, sh-MAFG-AS1#2 and sh-MAFG-AS1#3) and sh-NC were synthesized from Sangon Biotech (Shanghai, China). For overexpression of miR-3196, miR-3196 mimics and NC mimics were transfected into HCC cells. For overexpression of OTX1, pcDNA3.1 vector (Genechem Company, Shanghai, China) was subcloned with OTX1 to construct pcDNA3.1/OTX1 vector. Empty pcDNA3.1 vector was employed as a negative control. Cell transfection was performed according to the instructions of Lipofectamine 2000 (Invitrogen, Carlsbad, CA, USA). After 48 h of transfection, the cells were collected for subsequent experiments.

### Cell Proliferation Assay

The viability of MHCC97-H and Huh7 cells was detected in strict accordance with cell counting kit-8 (CCK-8) assay. Briefly, transfected cells were first seeded into 96-well plates, and cultured for 0 h, 24 h, 48 h, 72 h, and 96 h, respectively. At appointed time points, 10  $\mu$ L of CCK-8 reagent (Dojindo Molecular Technologies, Kumamoto, Japan) was added to each well, followed by incubation for 4 h in the dark. Absorbance at 450 nm was finally evaluated by a micro-plate reader.

### Transwell Assay

The migration and invasion of HCC cells were examined by the use of chambers coated or non-coated with Matrigel, respectively. Briefly, cells were plated into the upper chamber with serum-free DMEM. Meanwhile, complete DMEM with 10% FBS was added to the lower chamber as chemoattractant. After 24 h of incubation, cells migrated or invaded through the membrane to the lower chamber were stained with 0.1% crystal violet. Finally, the number of migrated or invaded cells was counted under an inverted microscope

(Olympus, Tokyo, Japan). 5 fields of view were randomly selected for each sample.

**RNA Binding Protein Immunoprecipitation (RIP) Assay**

RIP assay was conducted according to the instructions of a Magna RIP RNA-Binding Protein Immunoprecipitation reagent kit (Merck Millipore, Billerica, MA, USA). HCC cells were lysed in RIP buffer and incubated with magnetic beads conjugated to Ago2 antibody (ab32381; Abcam Inc., Cambridge, MA, USA) or IgG antibody (ab172730; 1:5000; Abcam Inc., Cambridge, MA, USA). Finally, immunoprecipitated RNAs were evaluated by real-time quantitative polymerase chain reaction (RT-qPCR).

**Real-Time Quantitative Polymerase Chain Reaction (RT-qPCR)**

Total RNAs in tissues and cells were extracted using TRIzol reagent (Invitrogen, Carlsbad, CA, USA). Complementary deoxyribose nucleic acid (cDNA) of MAFG-AS1 and OTX1 mRNA was produced with the RNA reverse transcription kit (Applied Biosystems, Foster City, CA, USA), while cDNA of miR-3196 was reversely transcribed by TaqMan miRNA Reverse Transcrip-

tion Kit (Applied Biosystems, Foster City, CA, USA). Glyceraldehyde 3-phosphate dehydrogenase (GAPDH) and U6 were used as internal references for MAFG-AS1 and OTX1, and miR-3196, respectively. The relative expression of genes was calculated by the  $2^{-\Delta\Delta Ct}$  method. Primer sequences used in this study were as follows: MAFG-AS1 forward: 5'-ATGACGACCCCAATAAAGGA-3', and reverse: 5'-CACCGACATGTTACCAGC-3'; miR-3196 forward: 5'-CCTGTGTATGCATCCTCGACTG-3', and reverse: 5'-CTGGCGTGTAATGGAGTCG-3'; OTX1 forward: 5'-CTGCTCTTCCTCAATCAATGG-3', and reverse: 5'-ACCCTGACTTGTCTGTTTCC-3'; GAPDH forward: 5'-ATGGGACGATGCTGGTACTGA-3', and reverse: 5'-TGCTGACAACCTTGAGTGAAAT-3'; U6 forward: 5'-CTCGCTTCGGCAGCACA-3', and reverse 5'-AACGCTTCACGAATTTGCGT-3'. The other miRNAs primers were listed in Table I.

**Luciferase Report Gene Assay**

Fluorescent reporter vectors of pmirGLO were provided by Promega (Madison, WI, USA), and pmirGLO-MAFG-AS1-wild-type (WT), pmirGLO-OTX1-WT, pmirGLO-MAFG-AS1-mutant (Mut), and pmirGLO-OTX1-Mut were con-

**Table I.** The primer primers of miRNAs (except miR-3196) that might bind with MAFG-AS1 were listed.

Gene	Primer primers
miR-642a-5p	forward: 5'-AAATGTGTCTTGGGGTGGGG-3' reverse: 5'-AATGATGGCAGAGGCCGAG-3'
miR-143-3p	forward: 5'-CAGTGCTGCATCTGTGTC-3' reverse: 5'-TGCAGAACAACTTCTCTTCCT-3'
miR-24-3p	forward: 5'-CCGGTGCCTACTGAGCTGAT-3' reverse: 5'-GTTCTGCTGAACTGAGCCA-3'
miR-744-5p	forward: 5'-CTTCCCTTGGAAATGATCTGA-3' reverse: 5'-TTATGAGAGTGGCAACAG-3'
miR-4640-5p	forward: 5'-CAGCTGGTGGGTGGGAAGTA-3' reverse: 5'-CTGTGGGCCAGGAAACAGG-3'
miR-4770	forward: 5'-GCTTTTTAAATGGGGCACAG-3' reverse: 5'-CGAAATTGGCGATACGTGA-3'
miR-5586-5p	forward: 5'-GCTTTTTAAATGGGGCACAG-3' reverse: 5'-CGAAATTGGCGATACGGGT-3'
miR-147b	forward: 5'-GTGGAAACATTCTGCACAAA-3' reverse: 5'-TTCCGGCAGGGCATATGGA-3'
miR-1270	forward: 5'-TGCAAAGAGCCACATAGAAGAT-3' reverse: 5'-CTGGAGATATGGAAGAGCTGTGT-3'
miR-650	forward: 5'-TGGGGTCTCAGGAGGCAG-3' reverse: 5'-TGAGTGAGGAGGGTGAGGAG-3'
miR-18a-5p	forward: 5'-TCCGAGATAGACGTGATCTA-3' reverse: 5'-GTGCAGGGTCCGAGGT-3'
miR-18b-5p	forward: 5'-CCAGAAGGGGCATTTAGGGC-3' reverse: 5'-AGGTGCATCTAGTGCAGTTAGT-3'
miR-331-3p	forward: 5'-GAGCTGAAAGCACTCCCAA-3' reverse: 5'-CACACTTTGATGTTCCAGGA-3'

structed by Genepharma Company. Obtained pmirGLO-MAFG-AS1-wild-type (WT), pmirGLO-OTX1-WT, pmirGLO-MAFG-AS1-mutant (Mut), and pmirGLO-OTX1-Mut were co-transfected with miR-3196 mimics and NC mimics into HCC cell lines, respectively. 48 h after transfection, Luciferase activity of cells was detected in accordance with Dual-Luciferase Activity Assay Kit (Promega, Madison, WI, USA).

### **Nuclear-Cytoplasmic Fractionation**

Nuclear-cytoplasmic fractionation assay was performed with PARIS™ Kit (Invitrogen, Carlsbad, CA, USA). Briefly, HCC cells were lysed in cell fractionation buffer, and the supernatant was harvested. Then, the cell lysates were put into the cell fractionation buffer and centrifuged. Next, cell disruption buffer was supplemented to lyse cell nuclei. Separated RNA was finally determined by RT-qPCR. GAPDH or U6 were employed as internal controls.

### **Tubule Formation Assay**

Capillary tubule formation assay was implemented to determine the function of MAFG-AS1 on HCC angiogenesis. Briefly, Matrigel was supplemented into each well and allowed to solidify at 37°C for 1 h. Then, HCC cells were seeded into each well and incubated in supernatants of MAFG-AS. Tubule formation was finally observed under an inverted microscope (Olympus Corporation, Tokyo, Japan).

### **Immunohistochemistry (IHC) Assay**

Fresh tissues obtained from nude mice were first fixed in paraformaldehyde. Afterwards, fixed tissue samples were dehydrated in ethanol solutions, inset in paraffin. Next, these specimens were cut into 4- $\mu$ m thickness sections and incubated with primary antibodies against Ki67 (Santa Cruz Biotechnology, Santa Cruz, CA, USA), PCNA (Santa Cruz Biotechnology, Santa Cruz, CA, USA), E-cadherin, or N-cadherin overnight at 4°C. On the next day, the sections were incubated with horseradish peroxidase (HRP)-conjugated secondary antibodies. Finally, the sections were visualized using OLYMPUSBX-41 microscope (Olympus, Tokyo, Japan).

### **Xenograft Assay in Mice**

This experiment was approved by the Ethics Committee of Fudan University. Nude mice were bought from Shi Laike Company (Shanghi, China), and fed in the laboratory of Fudan University. Cells transfected with sh-MAFG-AS1#1 or sh-

NC or sh-MAFG-AS1#1+pcDNA3.1/OTX1 were subcutaneously injected into the flanks of nude mice. The growth of tumors was recorded every 4 days. After 28 days of inoculation, short-acting but powerful sodium pentobarbital was injected into the abdomens of nude mice. Next, the breath of nude mice was ceased by the euthanasia treatment. After the mice were killed, tumors were resected for subsequent *in vivo* analysis.

### **Statistical Analysis**

Statistical Product and Service Solutions (SPSS) 21.0 statistical software (IBM Cop. Armonk, NY, USA) was used for all statistical analysis. Data were expressed as mean  $\pm$  standard deviation from at least three independent experiments. Student's *t*-test was used to compare the difference between two groups. One-way analysis of variance was applied for comparison among different groups. The correlation between MAFG-AS1 and miR-3196, MAFG-AS1 and OTX1 as well as miR-3196 and OTX1 was analyzed with Pearson's correlation analysis.  $p < 0.05$  was considered statistically significant.

## **Results**

### **The Expression of MAFG-AS1 Was Elevated in HCC Tissues and Cells**

To investigate the role of MAFG-AS1 in HCC, its expression in HCC tissues and cells was first evaluated by RT-qPCR. The results showed that MAFG-AS1 was highly expressed in HCC tissues and cell lines (HCCLM3, Hep3B, Huh7 and MHCC97-H) ( $p < 0.05$ , Figure 1A). MHCC97-H and Huh7 cells presented higher expression of MAFG-AS1, which were selected for subsequent experiments. Subsequently, MAFG-AS1 was knocked down in MHCC97-H and Huh7 cells, disclosing the downregulation of MAFG-AS1 *in vitro* (Figure 1B). Sh-MAFG-AS1#1 and sh-MAFG-AS1#2 showed better knockdown efficiency of MAFG-AS1, which were chosen for the following loss-of-function assays.

### **Deficiency of MAFG-AS1 Suppressed the Progression of HCC**

CCK-8 assay was used to detect the proliferation ability of HCC cells. The results indicated that MAFG-AS1 deficiency significantly repressed the proliferation of HCC cells ( $p < 0.05$ , Figure 1C). Similarly, transwell assay displayed that the number of migrated and invaded HCC

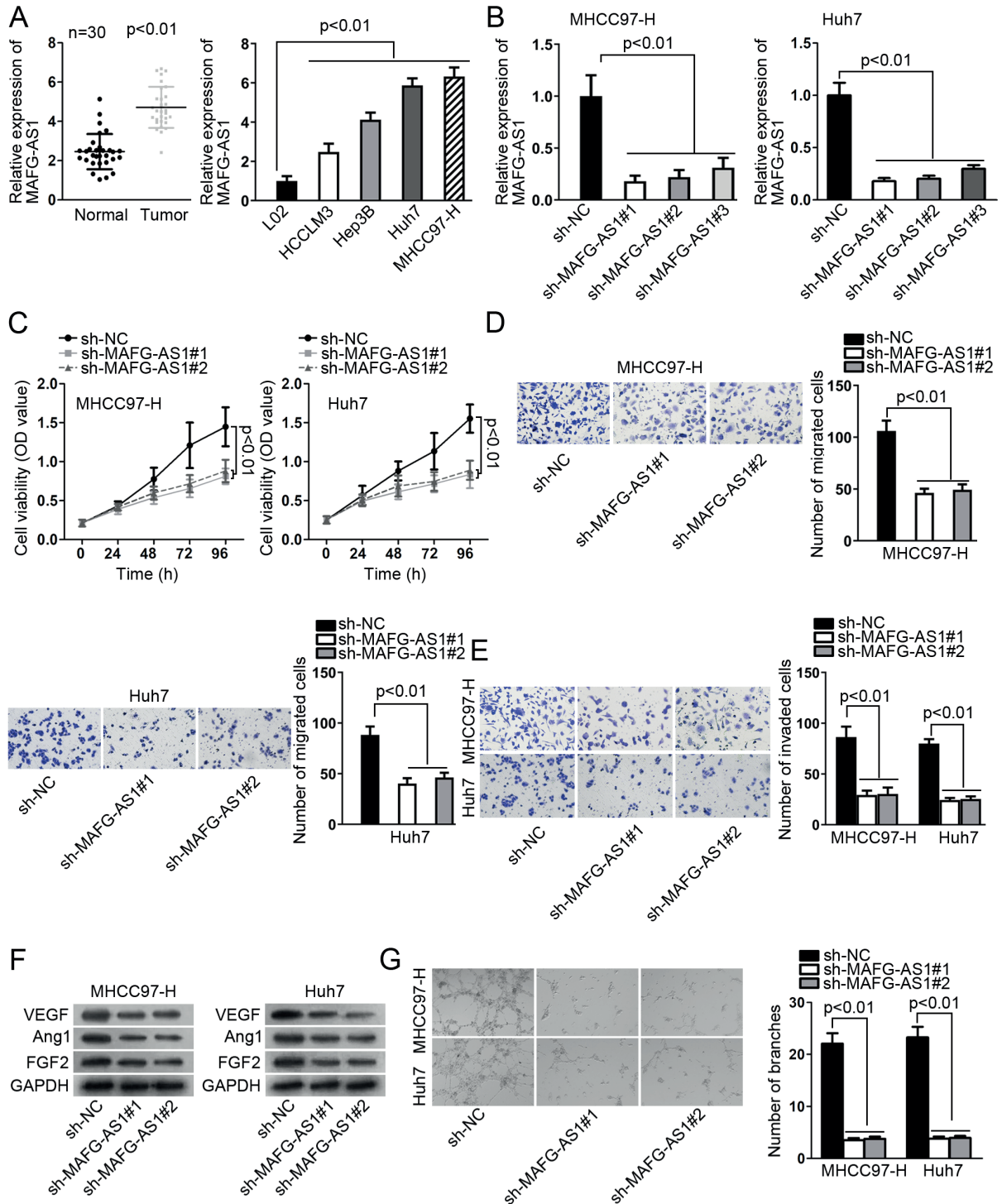


**Figure 1.** The expression of MAFG-AS1 was elevated in HCC tissues and cells. Deficiency of MAFG-AS1 suppressed the progression of HCC. **A**, RT-qPCR disclosed the expression of MAFG-AS1 in HCC tissues and adjacent non-tumor tissues, as well as in HCC cell lines and normal liver cells.  $p < 0.01$ . **B**, RT-qPCR exhibited the expression of MAFG-AS1 in HCC cells.  $p < 0.01$ . **C**, CCK-8 assay illustrated the proliferation of HCC cells, (magnification: 40 $\times$ ). **D-E**, Transwell assay manifested the migration and invasion of HCC cells.  $p < 0.01$ , (magnification: 40 $\times$ ). **F**, Western blot assay demonstrated angiogenesis ability in HCC cells. **G**, Tubule formation assay illustrated capillary tubule formation capacity in HCC cells  $p < 0.01$ , (magnification: 10 $\times$ ).

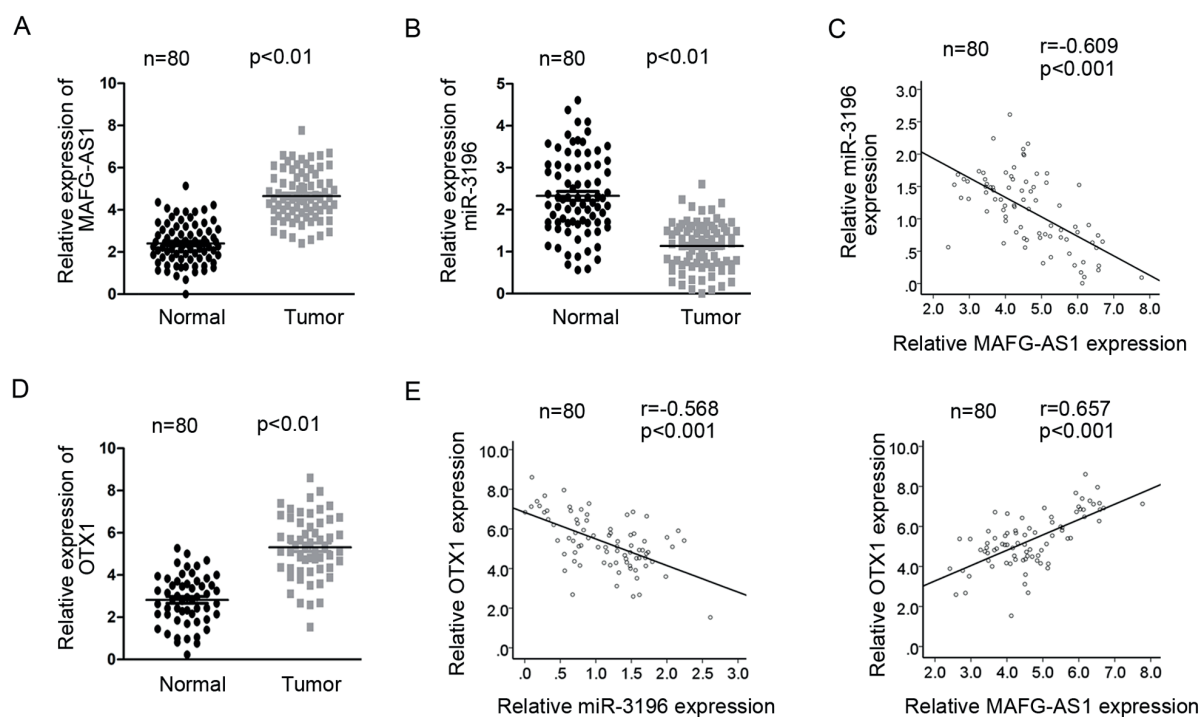


**Figure 2.** There was a correlation between the expressions of MAFG-AS1, miR-3196 and OTX1. **A-B**, The expression of MAFG-AS1 and miR-3196 in HCC tissues and adjacent non-tumor tissues was detected by RT-qPCR.  $p < 0.01$ . **C**, Pearson's correlation analysis showed the correlation between MAFG-AS1 and miR-3196.  $p < 0.001$ . **D**, The expression of OTX1 in HCC tissues and adjacent non-tumor tissues was detected by RT-qPCR.  $p < 0.01$ . **E**, Pearson's correlation analysis proved the correlation between OTX1 and MAFG-AS1/miR-3196.  $p < 0.001$ .

cells decreased significantly by MAFG-AS1 depletion ( $p < 0.05$ , Figure 1D, E). Moreover, Western blot assay demonstrated that MAFG-AS1 down-regulation significantly reduced the protein level of angiogenesis-related proteins (VEGF, Ang1 and FGF2) ( $p < 0.05$ , Figure 1F). Tubule formation assay illustrated that MAFG-AS1 attenuated capillary tubule formation in HCC cells (Figure 1G). In conclusion, MAFG-AS1 down-regulation inhibited cell proliferation, migration, invasion and tumor angiogenesis in HCC.

### **MAFG-AS1 Functioned as a Sponge for MiR-3196**

To elucidate the role of MAFG-AS1 in HCC, its expression in HCC tissues and cells was evaluated by RT-qPCR. The results manifested that the expression of MAFG-AS1 was predominantly higher in HCC tissues than that in adjacent non-tumor tissues ( $p < 0.05$ , Figure 2A). RT-qPCR detected the expression of miR-3196 in HCC tissues and cells as well. The results indicated that miR-3196 was lowly expressed in HCC tissues and cells ( $p < 0.05$ , Figure

2B). Pearson's correlation analysis disclosed that there was a negative correlation between MAFG-AS1 and miR-3196 in HCC (Figure 2C). Theoretically, lncRNAs, which are mainly located in the cytoplasm, can serve as competing endogenous RNAs (ceRNAs) to sponge miRNAs. Nuclear-cytoplasmic fractionation was implemented to investigate the localization of MAFG-AS1. The results demonstrated that MAFG-AS1 was preferentially situated in the cytoplasm (Figure 3A). Accordingly, bioinformatics analysis of starBase was employed to explore the miRNAs that could bind with MAFG-AS1 in HCC. RT-qPCR was utilized to examine the expression of miRNAs by co-transfection with sh-MAFG-AS1#1. The results showed that miR-3196 expression increased significantly in both cells ( $p < 0.05$ , Figure 3B). Therefore, miR-3196 was further explored in the present study. The potential binding site for MAFG-AS1 and miR-3196 was presented in Figure 3C. Subsequent RT-qPCR results showed that miR-3196 expression was notably reduced in both HCC tissues and HCC cells ( $p < 0.05$ , Fig-

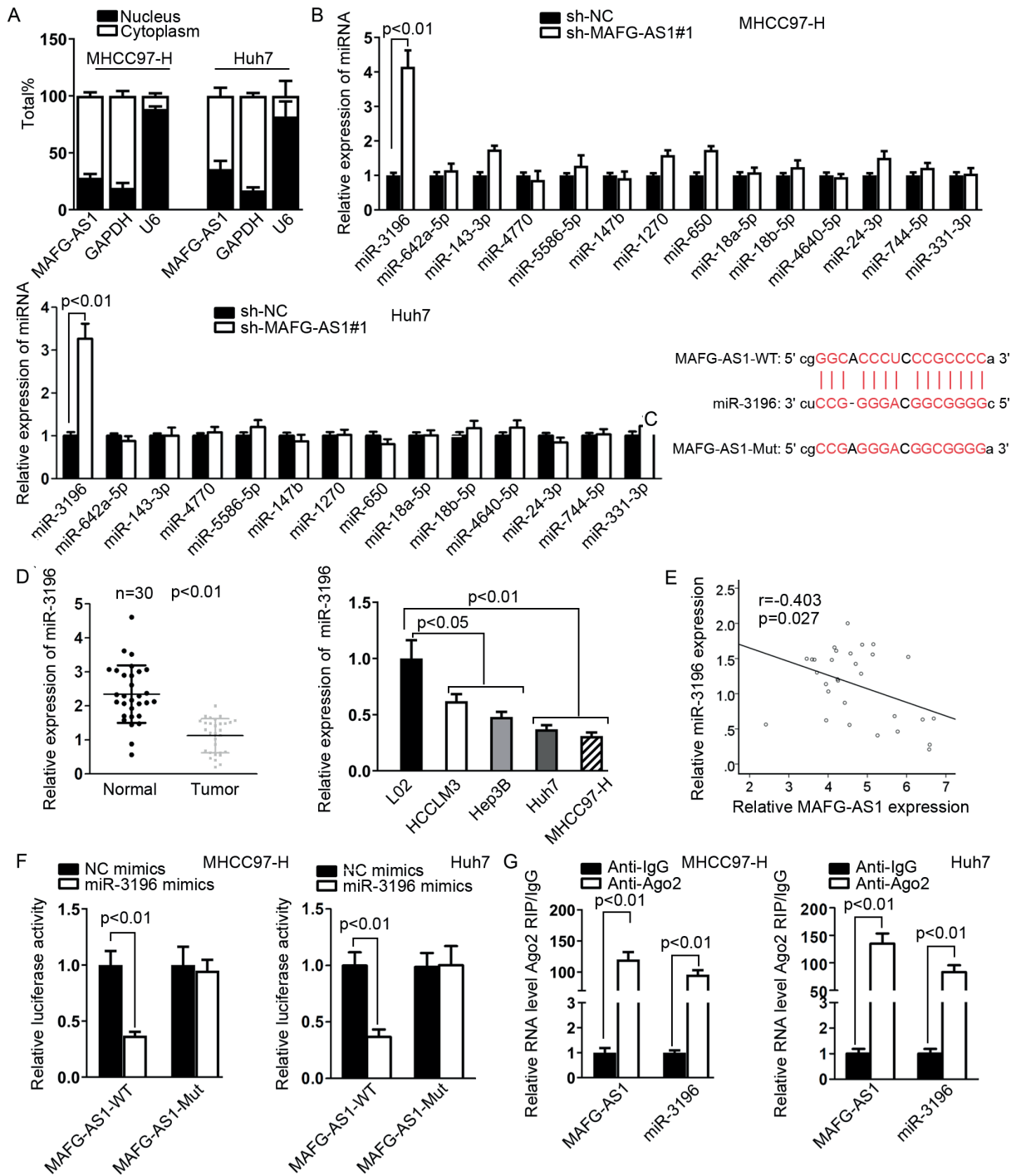


**Figure 3.** MAFG-AS1 functioned as a sponge for miR-3196. **A**, Nuclear-cytoplasmic fractionation assay was implemented to detect the location of MAFG-AS1 in cytoplasm. **B**, RT-qPCR was carried out to evaluate the expression of potential target miRNAs of MAFG-AS1.  $p < 0.01$ . **C**, The predicted binding site for MAFG-AS1 and miR-3196. **D**, The expression of miR-3196 in HCC tissues and adjacent non-tumor tissues, as well as in HCC cell lines and normal liver cells was determined by RT-qPCR.  $p < 0.05$ ,  $p < 0.01$ . **E**, Pearson's correlation analysis was used to investigate the correlation between MAFG-AS1 and miR-3196.  $p = 0.027$ . **F-G**, Luciferase reporter gene assay and RIP assay were applied to verify whether MAFG-AS1 could bind with miR-3196.  $p < 0.01$ .

ure 3D). Pearson's correlation analysis disclosed that there was a negative correlation between MAFG-AS1 and miR-3196 (Figure 3E). Additionally, transfection of miR-3196 mimics distinctly inhibited the Luciferase activity of pmirGLO-MAFG-AS1-WT ( $p < 0.05$ ). However, pmirGLO-MAFG-AS1-Mut exhibited no evident response to miR-3196 ( $p > 0.05$ , Figure 3F), suggesting that MAFG-AS1 could sponge miR-3196. RIP assay was carried out to validate whether MAFG-AS1 and miR-3196 were both implicated in the RNA-induced silencing complex (RISC). The results showed that both MAFG-AS1 and miR-3196 were accumulated in anti-Ago2 immunoprecipitates in comparison with anti-IgG group ( $p < 0.05$ , Figure 3G). Taken together, MAFG-AS1 functioned as a sponge for miR-3196 in HCC.

#### ***OTX1 Was a Downstream Target of MiR-3196***

Numerous studies have unveiled that miRNAs sponged by lncRNAs can interact with target mRNAs. As the above findings have verified the sponging function of MAFG-AS1 to miR-3196, the downstream target of miR-3196 in HCC needs to be clarified. Based on microT, miRmap and PicTar, there were two potential downstream targets (BBC3 and OTX1) for miR-3196 (Figure 4A, 4B). RT-qPCR showed that overexpression of miR-3196 significantly decreased OTX1 expression ( $p < 0.05$ ). However, no significant changes were observed in BBC3 expression in both cells ( $p > 0.05$ , Figure 4C). Therefore, OTX1 was chosen for further investigation. As shown in Figure 4D, there was a potential binding site between miR-3196 and OTX1. Subsequently, the expression of OTX1 in HCC tissues and adjacent non-tumor tissues was explored. The results indicated that OTX1 expression increased remarkably in HCC tissues compared with adjacent non-tumor tissues ( $p < 0.05$ , Figure 4E). OTX1 was highly expressed in HCC cells as well ( $p < 0.05$ , Figure 4F). Moreover, there was a negative correlation between miR-3196 and OTX1, but a positive correlation between MAFG-AS1 and OTX1 (Figure 4G). In addition, overexpression of miR-3196 reduced the Luciferase activity of pmirGLO-OTX1-WT ( $p < 0.05$ ). However, no significant change was observed in the Luciferase activity of pmirGLO-OTX1-Mut ( $p > 0.05$ , Figure 4H). RIP assay manifested that MAFG-AS1, miR-3196 and OTX1 were all enriched in anti-Ago2 group but not in anti-IgG group (Figure 4I). To sum up, OTX1 was a downstream target of miR-3196.

#### ***MAFG-AS1 Aggravated the Progression of HCC Via Targeting MiR-3196/OTX1 Axis***

We probed whether MAFG-AS1 aggravated the progression of HCC *via* targeting miR-3196/OTX1 axis through rescue assays. pcDNA3.1/OTX1 was transfected into MHCC97-H cells to up-regulate OTX1 expression (Figure 5A). CCK-8 assay indicated that overexpression of OTX1 could counteract the inhibition of MAFG-AS1 silence on the proliferation of MHCC97-H cells (Figure 5B). Transwell assay illustrated that up-regulation of OTX1 could recover the inhibitory function of MAFG-AS1 attenuation on cell migration and invasion (Figure 5C, 5D). Moreover, down-regulated expression of angiogenesis-related proteins (VEGF, Ang1 and FGF2) owing to MAFG-AS1 inhibition was reversed by OTX1 upregulation. Overexpression of OTX1 offset the suppressive effect of MAFG-AS1 depletion on the protein expression of OTX1 (Figure 5E). MAFG-AS1 attenuated capillary tubule formation in HCC cells, while this effect was abolished by enhancement of OTX1 (Figure 5F). Next, *in vivo* assays were employed to further verify the regulatory role of MAFG-AS1. As shown in Figure 6A-6C, upregulation of OTX1 could restore the repressive effect of MAFG-AS1 knockdown on tumor growth, volume, and weight. Likewise, OTX1 overexpression could rescue the effect of MAFG-AS1 silence on the expression of Ki67, PCNA, E-cadherin and N-cadherin. These results suggested that up-regulated OTX1 could counteract the restraining influence of MAFG-AS1 deficiency on cell proliferation and EMT process (Figure 6D). In summary, MAFG-AS1 promoted the progression of HCC *via* targeting miR-3196/OTX1 axis.

## **Discussion**

Increasing studies have illustrated that a large number of lncRNAs are aberrantly expressed in HCC. These lncRNAs participate in the tumorigenesis and development of HCC by serving as ceRNAs. Of note, lncRNA AGAP2-AS1 facilitates the proliferation and metastasis of HCC cells *via* upregulating ANXA11 expression through sponging miR-16-5p<sup>17</sup>. lncRNA MIR31HG suppresses HCC proliferation and metastasis *via* sponging miR-575 to regulate ST7L expression<sup>18</sup>. lncRNA KTN1-AS1 facilitates the progression of HCC *via* regulating miR-23c/ERBB2IP axis<sup>19</sup>.



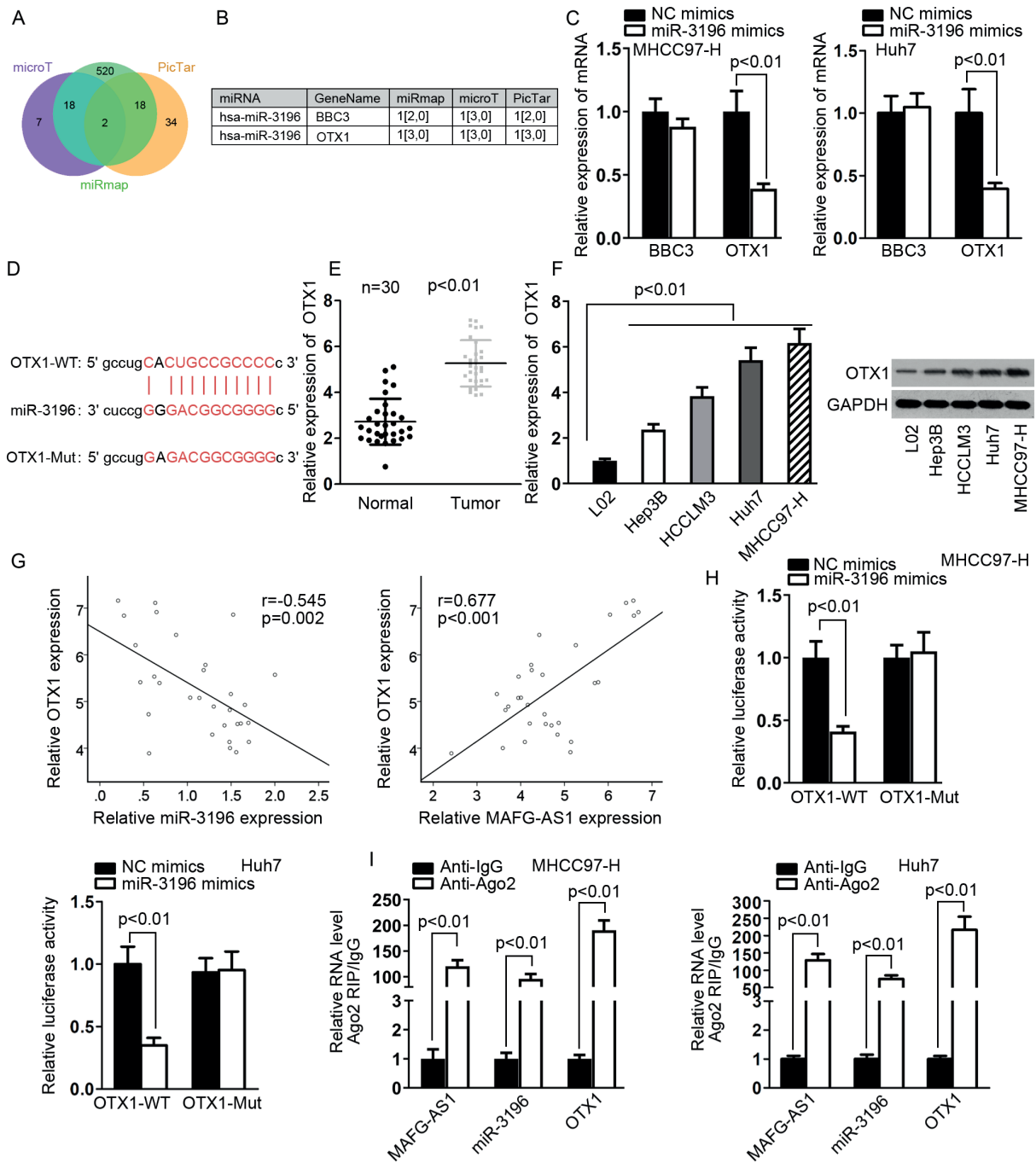


**Figure 4.** OTX1 was a downstream target of miR-3196. **A**, Candidate genes targeted by miR-3196 were shown by the Venn diagram. **B**, Two candidate genes targeted by miR-3196 were presented. **C**, RT-qPCR displayed the expression of the two candidate genes.  $p < 0.01$ . **D**, The predicted binding site for miR-3196 and OTX1 was exhibited. **E-F**, The expression of OTX1 in HCC tissues and adjacent non-tumor tissues, as well as in HCC cell lines and normal liver cells was detected by RT-qPCR.  $p < 0.01$ . **G**, Pearson's correlation analysis was employed to investigate the correlation between miR-3196 and OTX1, as well as MAFG-AS1 and OTX1.  $p = 0.002$  (left),  $p < 0.01$  (right). **H-I**, Luciferase reporter gene assay and RIP assay were conducted to confirm whether miR-3196 could bind with OTX1.  $p < 0.01$ .

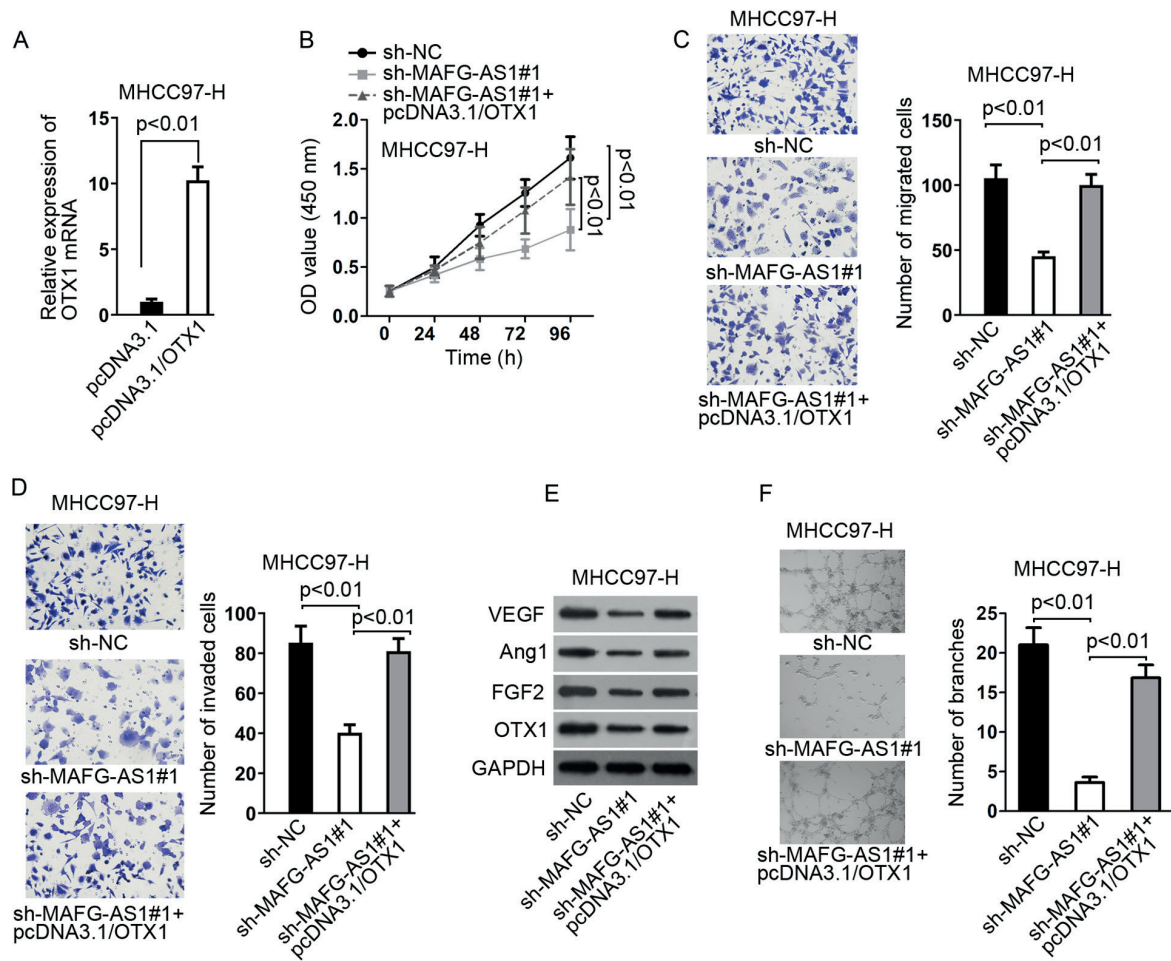


**Figure 5.** MAFG-AS1 aggravated the progression of HCC *via* targeting miR-3196/OTX1 axis. **A**, Transfection efficiency of OTX1 was tested by RT-qPCR.  $p < 0.01$ . **B**, The changes in the proliferation of MHCC97-H cells were determined by CCK-8 assay.  $p < 0.01$ . **C-D**, The changes in the migration and invasion of MHCC97-H cells were explored by transwell assay.  $p < 0.01$ , (magnification: 40 $\times$ ) **E**, Western blot assay demonstrated angiogenesis ability in MHCC97-H cells. **F**, Tubule formation assay determined the capillary tubule formation capacity in MHCC97-H cells.  $p < 0.01$ , (magnification: 10 $\times$ ).

LncRNA CRNDE aggravates the proliferation, migration and invasion of HCC cells *via* targeting miR-217/MAPK1 axis<sup>20</sup>. Existing literature has clarified that lncRNA MAFG-AS1 can act as a ceRNA to promote the progression of human cancers, such as lung adenocarcinoma cell<sup>14</sup>, breast carcinoma<sup>15</sup> and colorectal cancer<sup>16</sup>. Therefore, it is of great possibility that MAFG-AS1 mediates HCC development through the ceRNA network. In the current study, MAFG-AS1 was highly expressed in HCC tissues and cells. Biological function assay indicated that MAFG-AS1 deficiency abundantly alleviated the proliferation, migration and invasion as well as angiogenesis of HCC cells. All these findings demonstrated that MAFG-AS1 could promote the progression of HCC.

MicroRNAs (miRNAs) are a kind of endogenous small noncoding RNA molecules with 19-26 nucleotides in length. They have been confirmed to negatively regulate the expression of target genes<sup>21</sup>. A growing number of studies have attested that lncRNAs exert their functions through interacting with miRNAs<sup>22-24</sup>. However, whether MAFG-AS1 contributes to HCC *via* interaction with miRNA remains to be investigated. Recent reports have uncovered that miR-3196 elicits repressive effect on tumor progression. MiR-3196 overexpression inhibits the proliferation and promotes the apoptosis of breast cancer cells *via* targeting ERBB3<sup>25</sup>. MiR-3196 was lowly expressed in gastric cancer and was negatively regulated by lncRNA ADPGK-AS1<sup>26</sup>. In the pres-

ent study, bioinformatics prediction and molecular assays demonstrated that miR-3196 could bind with MAFG-AS1 in HCC. Moreover, there was a negative association between MAFG-AS1 and miR-3196 in HCC. All the results suggested that MAFG-AS1 directly targeted miR-3196 in HCC.

Orthodenticle homolog 1 (OTX1) has been uncovered to be tightly correlated with the progression of several malignancies. Of note, inhibition of OTX1 suppresses the proliferation, migration and invasion of gastric cancer cells<sup>27</sup>. OTX1 contributes to the progression of colorectal cancer by promoting epithelial-mesenchymal transition<sup>28</sup>. The present study verified that miR-3196 could target OTX1. OTX1 was highly expressed in HCC tissues and cells. OTX1 was negatively associated with miR-3196 and positively associated with MAFG-AS1. Rescue assays *in vitro*

and *in vivo* further delineated that overexpression of OTX1 could recover the suppressive effect of MAFG-AS1 silence on HCC progression.

### Conclusions

MAFG-AS1 facilitated the progression of HCC *via* targeting miR-3196/OTX1 axis. Ouyang et al<sup>29</sup> uncovered high expression of MAFG-AS1 in HCC tissues and cells, and has confirmed its role in promoting the proliferation, migration and invasion of HCC cells. In the present study, we further investigated target miRNAs of MAFG-AS1, and validated the ceRNA mechanism of MAFG-AS1 in HCC. MAFG-AS1 exerted its oncogenic role in HCC progression *via* regulating OTX1 expression. The novelty was that the ceRNA network of MAFG-

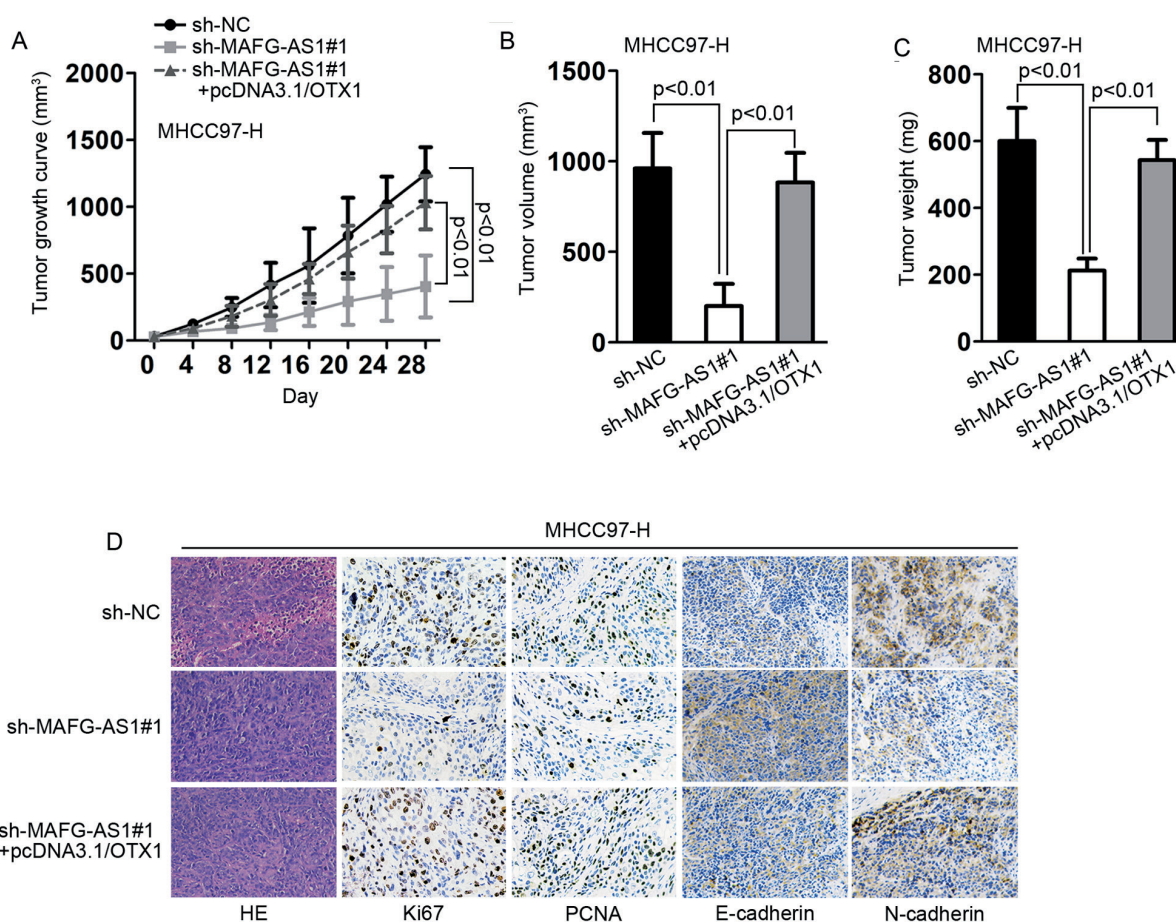


**Figure 6.** Downregulation of MAFG-AS1 suppressed the progression of HCC *in vivo*. **A**, Tumor growth curve was depicted when mice were injected with MHCC97-H cells transfected with different plasmids.  $p < 0.001$ . **B**, Tumor volume ( $p < 0.001$ ) and **C**, Weight ( $p < 0.001$ ). **D**, Immunohistochemistry assay was performed to evaluate the changes in the expression of ki67, PCNA, E-cadherin and N-cadherin, (magnification: 400 $\times$ ).

AS1 exists in HCC and MAFG-AS1 is expected to become a new biomarker for HCC treatment.

### Funding Acknowledgements

Commission of Science Technology of Minhang District (2019MHZ079 to ZQH); Minhang scientific research found projects grant (2017MHJC02 to ZQH).

### Conflict of Interest

The Authors declare that they have no conflict of interests.

## References

- 1) SIA D, VILLANUEVA A, FRIEDMAN SL, LLOVET JM. Liver cancer cell of origin, molecular class, and effects on patient prognosis. *Gastroenterology* 2017; 152: 745-761.
- 2) SIEGEL RL, MILLER KD, JEMAL A. Cancer statistics, 2017. *CA Cancer J Clin* 2017; 67: 7-30.
- 3) VENOOK AP, PAPANDREOU C, FURUSE J, DE GUEVARA LL. The incidence and epidemiology of hepatocellular carcinoma: a global and regional perspective. *Oncologist* 2010; 15 Suppl 4: 5-13.
- 4) JIAO HK, XU Y, LI J, WANG W, MEI Z, LONG XD, CHEN GO. Prognostic significance of Cbx4 expression and its beneficial effect for transarterial chemoembolization in hepatocellular carcinoma. *Cell Death Dis* 2015; 6: e1689.
- 5) GOLFIERI R, CAPPELLI A, CUCCHETTI A, PISCAGLIA F, CARPENZANO M, PERI E, RAVAIOLI M, D'ERRICO-GRIGIONI A, PINNA AD, BOLONDI L. Efficacy of selective transarterial chemoembolization in inducing tumor necrosis in small (<5 cm) hepatocellular carcinomas. *Hepatology* 2011; 53: 1580-1589.
- 6) CUCCHETTI A, DJULBEGOVIC B, TSALATSANIS A, VITALE A, HOZO I, PISCAGLIA F, CESCO M, ERCOLANI G, TUCI F, CILLO U, PINNA AD. When to perform hepatic resection for intermediate-stage hepatocellular carcinoma. *Hepatology* 2015; 61: 905-914.
- 7) FORNER A, HESSHEIMER AJ, ISABEL RM, BRUIX J. Treatment of hepatocellular carcinoma. *Crit Rev Oncol Hematol* 2006; 60: 89-98.
- 8) WANG KC, CHANG HY. Molecular mechanisms of long noncoding RNAs. *Mol Cell* 2011; 43: 904-914.
- 9) PONTING CP, OLIVER PL, REIK W. Evolution and functions of long noncoding RNAs. *Cell* 2009; 136: 629-641.
- 10) LING J, WANG F, LIU C, DONG X, XUE Y, JIA X, SONG W, LI Q. FOXO1-regulated lncRNA LINC01197 inhibits pancreatic adenocarcinoma cell proliferation by restraining Wnt/beta-catenin signaling. *J Exp Clin Cancer Res* 2019; 38: 179.
- 11) MIAO L, LIU HY, ZHOU C, HE X. LINC00612 enhances the proliferation and invasion ability of bladder cancer cells as ceRNA by sponging miR-590 to elevate expression of PHF14. *J Exp Clin Cancer Res* 2019; 38: 143.
- 12) GAO R, ZHANG N, YANG J, ZHU Y, ZHANG Z, WANG J, XU X, LI Z, LIU X, LI Z, LI J, KONG C, BI J. Long non-coding RNA ZEB1-AS1 regulates miR-200b/FSCN1 signaling and enhances migration and invasion induced by TGF-beta1 in bladder cancer cells. *J Exp Clin Cancer Res* 2019; 38: 111.
- 13) DONG S, WANG R, WANG H, DING Q, ZHOU X, WANG J, ZHANG K, LONG Y, LU S, HONG T, REN H, WONG K, SHENG X, WANG Y, ZENG Y. HOXD-AS1 promotes the epithelial to mesenchymal transition of ovarian cancer cells by regulating miR-186-5p and PIK3R3. *J Exp Clin Cancer Res* 2019; 38: 110.
- 14) SUI Y, LIN G, ZHENG Y, HUANG W. LncRNA MAFG-AS1 boosts the proliferation of lung adenocarcinoma cells via regulating miR-744-5p/MAFG axis. *Eur J Pharmacol* 2019; 859: 172465.
- 15) LI H, ZHANG GY, PAN CH, ZHANG XY, SU XY. LncRNA MAFG-AS1 promotes the aggressiveness of breast carcinoma through regulating miR-339-5p/MMP15. *Eur Rev Med Pharmacol Sci* 2019; 23: 2838-2846.
- 16) CUI S, YANG X, ZHANG L, ZHAO Y, YAN W. LncRNA MAFG-AS1 promotes the progression of colorectal cancer by sponging miR-147b and activation of NDUFA4. *Biochem Biophys Res Commun* 2018; 506: 251-258.
- 17) LIU Z, WANG Y, WANG L, YAO B, SUN L, LIU R, CHEN T, NIU Y, TU K, LIU Q. Long non-coding RNA AGAP2-AS1, functioning as a competitive endogenous RNA, upregulates ANXA11 expression by sponging miR-16-5p and promotes proliferation and metastasis in hepatocellular carcinoma. *J Exp Clin Cancer Res* 2019; 38: 194.
- 18) YAN S, TANG Z, CHEN K, LIU Y, YU G, CHEN Q, DANG H, CHEN F, LING J, ZHU L, HUANG A, TANG H. Long noncoding RNA MIR31HG inhibits hepatocellular carcinoma proliferation and metastasis by sponging microRNA-575 to modulate ST7L expression. *J Exp Clin Cancer Res* 2018; 37: 214.
- 19) ZHANG L, WANG L, WANG Y, CHEN T, LIU R, YANG W, LIU Q, TU K. LncRNA KTN1-AS1 promotes tumor growth of hepatocellular carcinoma by targeting miR-23c/ERBB2IP axis. *Biomed Pharmacother* 2019; 109: 1140-1147.
- 20) WANG H, KE J, GUO Q, BARNABO NK, YANG P, MA K. Long non-coding RNA CRNDE promotes the proliferation, migration and invasion of hepatocellular carcinoma cells through miR-217/MAPK1 axis. *J Cell Mol Med* 2018; 22: 5862-5876.
- 21) LEWIS BP, BURGE CB, BARTEL DP. Conserved seed pairing, often flanked by adenosines, indicates that thousands of human genes are microRNA targets. *Cell* 2005; 120: 15-20.
- 22) ZHANG S, ZHANG X, SUN Q, ZHUANG C, LI G, SUN L, WANG H. LncRNA NR2F2-AS1 promotes tumorigenesis through modulating BMI1 expression by targeting miR-320b in non-small cell lung cancer. *J Cell Mol Med* 2019; 23: 2001-2011.
- 23) LI H, GUO X, LI Q, RAN P, XIANG X, YUAN Y, DONG T, ZHU B, WANG L, LI F, YANG C, MU D, WANG D, XIAO C, ZHENG S. Long non-coding RNA 1308 promotes cell invasion by regulating the miR-124/ADAM 15 axis in non-small-cell lung cancer cells. *Cancer Manag Res* 2018; 10: 6599-6609.

- 24) ZONG L, SUN Q, ZHANG H, CHEN Z, DENG Y, LI D, ZHANG L. Increased expression of circRNA\_102231 in lung cancer and its clinical significance. *Biomed Pharmacother* 2018; 102: 639-644.
- 25) JI ZC, HAN SH, XING YF. Overexpression of miR-3196 suppresses cell proliferation and induces cell apoptosis through targeting ERBB3 in breast cancer. *Eur Rev Med Pharmacol Sci* 2018; 22: 8383-8390.
- 26) HUANG Z, YANG H. Upregulation of the long noncoding RNA ADPGK-AS1 promotes carcinogenesis and predicts poor prognosis in gastric cancer. *Biochem Biophys Res Commun* 2019; 513: 127-134.
- 27) QIN SC, ZHAO Z, SHENG JX, XU XH, YAO J, LU JJ, CHEN B, ZHAO GD, WANG XY, YANG YD. Downregulation of OTX1 attenuates gastric cancer cell proliferation, migration and invasion. *Oncol Rep* 2018; 40: 1907-1916.
- 28) YU K, CAI XY, LI Q, YANG ZB, XIONG W, SHEN T, WANG WY, LI YF. OTX1 promotes colorectal cancer progression through epithelial-mesenchymal transition. *Biochem Biophys Res Commun* 2014; 444: 1-5.
- 29) OUYANG H, ZHANG L, XIE Z, MA S. Long noncoding RNA MAFG-AS1 promotes proliferation, migration and invasion of hepatocellular carcinoma cells through downregulation of miR-6852. *Exp Ther Med* 2019; 18: 2547-2553.